

On-demand Electric Thrust Assistance for Muscle-powered Watercraft: PADDELEC

René Budich^a, Stephan Zipser, Jakob Doblaski and Jonas Seidel

Institute for Electric Mobility, University of Applied Sciences Dresden, Friedrich-List-Platz 1, Dresden, Germany

Keywords: Paddelec, Demand-oriented Support, Electric Mobility, BEV, Canoe, SUP, Watercraft, Boat Simulation.

Abstract: In the project *PADDELEC*, the implementation of an intelligent paddle (iPaddle) for controlling an electric assisted canoe was realized. This paddle is able to record the paddle force F_B of the blade with the help of measurement technology integrated in the paddle shaft. The recording of the paddle stroke is used as a control variable for operating an electric auxiliary drive in the boat. This is intended to provide on-demand thrust assistance to the athlete, analogous to an electrified bicycle (*pedelec*). Existing drive solutions on motorized boats offer the athlete the option of firmly specifying the desired thrust via a thrust lever or tiller. The *paddelec* has the aim to provide intelligent and dynamic thrust assistance to the athlete as needed. This is intended to preserve a natural driving feel, despite the auxiliary drive. A simulation model of the longitudinal dynamics of canoes, was developed to investigate various assistance strategies. The models were validated by extensive real driving tests. For this purpose, special hardware and software tools had to be created, which will be further developed in the future. With the simulation and the evaluation of the practical testing, it could be shown that thrust support for canoes can be very useful. The correct support strategy and support performance can vary greatly depending on which water conditions the boat will use and the sporting activity, so there is still a need for more research in this area.

1 INTRODUCTION

Water sports become more and more popular around the world. For example, there has been a steady and substantial increase in water touring by canoe (e.g. in countries like Canada, Sweden and Germany). The use of SUPs (Stand-Up-Boards) is also increasing for some years now (BMW, 2013).

In many cases water sports are performed at calm, near-natural coastal, inland waters or low-current rivers. However, it remains an outdoor sport where wind and water current (and/or tide) often require a powerful athlete.

To make this water sport available to a larger user group, a battery-electric propulsion support is an obvious suggestion. In case of bicycles, the idea of battery-electric support is known as *pedelec* (pedal electric cycle) and has been extraordinarily commercially successful in Europe.

As known, real live disturbances like wind and water current may affect the results of practical field tests substantially. For this reason, physically oriented models were developed to describe the response of a

boat to human and motor propulsion forces analytically. Model simulations in comparison to field tests are also presented later.


The project was largely driven by engineering students, who developed and implemented technical solutions for measuring and controlling the boat-drives and tested them in driving trials.

2 THE IDEA OF PADDELEC

The objective of the *paddelec* project is to develop a system which provides on-demand electric thrust assistance analogous to the established electric pedal assistance for bicycles: the propulsion input of the user is measured and supported electrically.

The basic principle of both technologies is identical.¹ In both cases, the mechanical input of the user (or less technical the desire for assistance) is measured with a torque or force sensor. In the case of canoeing, this is done with a paddle equipped with sensors. The measurements are processed by a control

¹This is why the name analogy to the *pedelec* was deliberately chosen.

^a  <https://orcid.org/0000-0002-9227-6834>

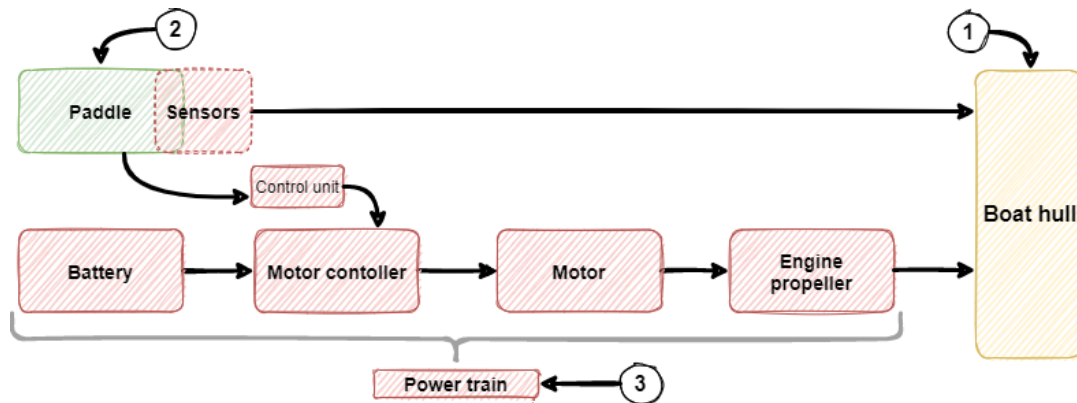


Figure 1: Block diagram of a paddleec.

unit, which drives the propulsion motor controller. Depending on the amount of power applied, the vehicle can thus be controlled by the driver.

The main focus is to provide a driving experience that is as natural as possible without the use of additional peripherals such as a throttle.

In a canoe, the propulsion force or power is transmitted with the help of a paddle. When paddling, the paddle is pushed against the water to move the canoe forward. To do this, the paddle blade is inserted into the water and the paddle shaft is pushed against it.

Fig. 1 shows the basic structure with the aid of a block diagram. The blocks shown in red are representing additional components which are necessary for implementing demand-oriented thrust support.

The paddle (Fig. 1 - ②) exerts a force F on the hull of the boat (Fig. 1 - ①) so that it moves longitudinally in the water. It should be noted here that the measured paddle force F_B can never be used to 100% for propulsion (paddle force $F_B \neq$ propulsive force F_T) (see also section 5.2.2).

In order to realize demand-oriented support, the force component in the direction of travel must be recorded. This is done with a special measuring paddle (iPaddle) which, among other things, has integrated sensors and strain gauges for position and force diagnostics. The recorded sensor values can be used to control an electric motor dynamically. The battery, motor controller, motor and propeller respectively jet are parts of the power train unit, which can be designed in different ways (Fig. 1 - ③).

3 STRUCTURE OF THE TEST VEHICLE

3.1 Boat Hull Grampus I

The Grampus I (a two-man kayak) from the Kaitts company shown in Fig. 2 was used for the test setup.

The hull is made entirely of plastic, which makes the boat very robust. This also makes it easy to implement modifications. The kayak has a wide hull cross-section, which provides high stability against tipping on the water and increased safety during test runs. Inside there is enough space for a traction battery, control unit and measurement equipment. The rear part of the kayak is sealed off watertight, allowing water-sensitive components and measurement technology to be accommodated via a hatch.



Figure 2: Boat hull - Grampus I (Kaitts Ltd., 2022).

3.2 iPaddle - Measuring Paddle

Fig. 3 shows a part of a classic double paddle typically used in popular sports. The developed iPaddle is equipped with force and position sensors and a wireless data transmission to the control unit.

The tensile force applied by the paddler causes a deformation of the paddle shaft. This bending is detected by a strain gauge and transmitted to the ADC (analog digital converter) as an electrical voltage change. The ADC amplifies the signal and converts it into a digital signal, which is transmitted to the control unit in the boat (Dr. Budich and Dabrazzi, 2020).

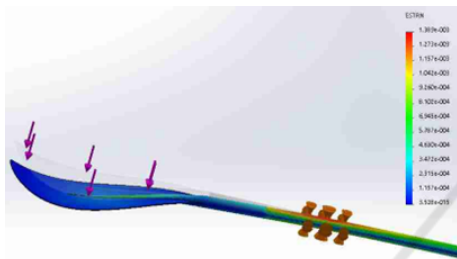


Figure 3: FEM analysis of the measuring paddle (Häse, 2020).

For the application of the strain gauges on the paddle, the area of highest stress should be selected. Therefore, the double paddle was statically loaded and then examined. The resulting stress curve over the paddle shaft was calculated before using a FE calculation (Finite elements method). It can be seen that the maximum bending moments and thus the maximum tensile and compressive stresses lie in the area of the grip point closest to the paddle blade (Fig. 3).

In order to determine all forces correctly, an exact position measurement is required, which is currently still under development.

For an initial estimate, it is sufficient to use a paddle factor to determine the propulsive force $F_{T thrust}$ from the measured force $F_{B blade}$ (F_B).

In further development we can use the measured paddle angle α to do the correction more accurately (see equation 1).

$$F_T(\alpha) = F_B \cdot K(\alpha) \quad (1)$$

3.3 Power Train

The basic structure of the *paddelec* is shown in Fig. 4. The structure consists of the components: Boat body (canoe) ①, iPaddle ②, battery ③, control unit ④ and the drive unit ⑤ (e.g. water jet drive).

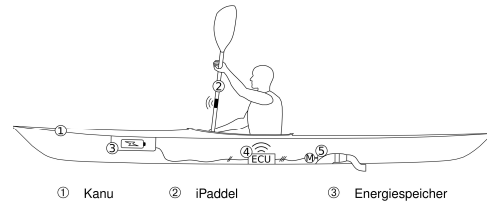


Figure 4: Basic structure *paddelec* (Pöschmann, 2020).

The electric auxiliary drive generates the desired additional thrust assistance through appropriate control. A waterjet propulsion system is favored as the drive unit because, unlike a propeller, it can be easily and safely integrated into the hull of the boat. It is also assumed to have a lower impact on the environment.

The waterjet drive for the test vehicle is made up of several individual components. All components were designed for additive manufacturing and 3D printed from polylactide plastic. The waterjet propulsion system is screwed to the fuselage and sealed using sealing compound. Fig. 5 shows the designed jet drive in installation position, Fig. 6 the underside of the hull with outlet opening and protective fins.

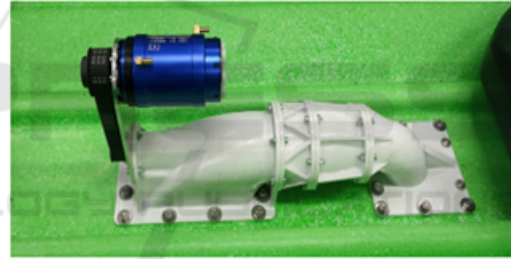


Figure 5: Constructed jet drive in installation position with motor and belt drive (Hauptmann, 2020).

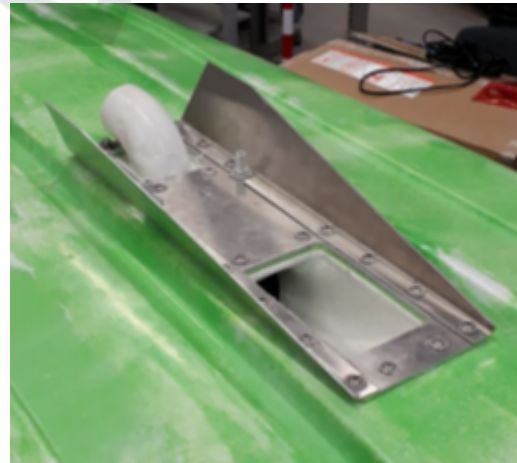


Figure 6: Bottom of the fuselage with protective fins and deflection of the outlet (Hauptmann, 2020).

In addition, investigations were carried out with



Figure 7: KDN-W703000 (Kedean, 2022).

a commercial drive solution (KDN-W703000) from Kedean (Fig. 7). A brushless DC motor is used here as the electric machine, while an impeller is used as the drive. These two components are installed in an aluminum housing as a combination. By using an impeller, the risk of injury is minimized in contrast to a propeller. Table 1 lists the available technical data for the drive.

Table 1: Technical data Kedean motor (Kedean, 2022).

technical characteristics	values
max. operating voltage	50 V
max. continuous current	75 A
max. power	4000 W
max. thrust	240 N
length	401 mm
weight	2.5 kg
impeller diameter	60 mm

3.4 Traction Battery

A battery solution from Aentron Energy Solutions was chosen to supply the system with energy. The company specializes in energy storage systems for the maritime sector. Important characteristics are shown in table 2.

The battery has an integrated battery management system (BMS), which provides overcharge and deep discharge protection, as well as temperature monitoring. Its robust aluminum housing and protection against dust and water make it a good solution for carrying out the measurement runs.

Table 2: Technical data battery (Aentron, 2022).

technical characteristics	values
capacity	20.3 Ah
energy	1023 Wh
continuous discharge power	3000 W (@ 60 A)
nominal voltage	50.4 V
operating voltage	42 V- 56 V
weight	9 kg
protection class	IP66

3.5 Electronic Control Unit - ECU

The developed control unit is based on an Arduino environment. The ECU acquires measurement data, processes it and sends corresponding signals to a motor controller. The necessary software algorithms were implemented with Matlab Simulink. Its also possible to log sensor data. The mode of operation is shown schematically in Fig. 8.

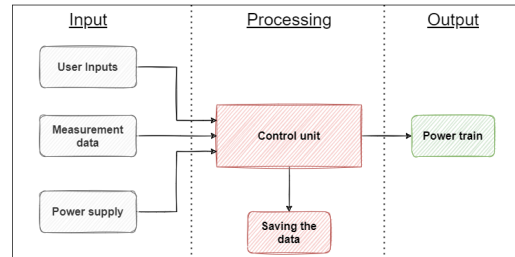


Figure 8: Basic scheme of ECU (Doblaski, 2021).

3.6 Housing and Peripherals

The control unit and the necessary peripherals must be securely housed on the boat. For this purpose, a housing was developed which protects the technology used from penetrating dirt and water (Fig. 9).

The D-Sub 9 connector ① serves as input for the paddle’s measurement data. The XT60 connector ② is used to connect the battery. The plastic cable gland ③ is used to guide the motor cable to the motor controller. The four-pole connector ④ is used to record the measured data from the battery. A switch ⑥ for switching the operating voltage of the Arduino on and off was mounted on the top. Two LEDs ⑦ serve as status and error indicators. Furthermore, a rotary incremental encoder ⑧ and a potentiometer ⑨ were attached to the top. With these, it is possible to change parameters while driving. In this way, different scenarios can be tested quickly during the measurement runs. To make the parameter changes visible, a display ⑩ was also mounted in the housing.



Figure 9: Housing for the electronic components (Doblaski, 2021).

4 SUPPORT STRATEGIES FOR THE PADDELEC

4.1 Conceptual Approaches

There are various strategies for demand-oriented support. Depending on the driver's wishes and objectives, the drive system implements a thrust depending on the support strategy selected. In the following, three selected basic strategies will be examined in more detail.

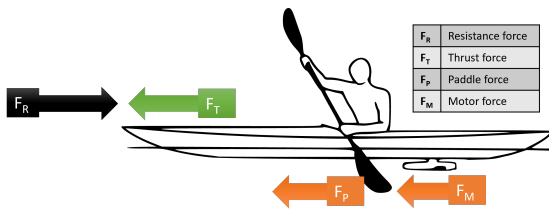


Figure 10: Basic forces for analysis support strategies.

The propulsive forces acting on the boat are shown in Fig. 10. They are divided into paddle forces F_P and motor forces F_M (orange arrows). The sum of the two forces is the total thrust force F_T (green arrow). This force acts against the resistance force F_R (black arrow).

4.2 Strategy 1 - Constant Support

In this strategy, the user is assisted by the drive with constant force. For this purpose, the force applied by the user to the paddle is averaged over several paddle strokes. The calculated force is then applied constantly by the drive for support (mode: tailwind).

Fig. 11 shows the individual force curves over time. The red line shows the progression of the force applied to the paddle.

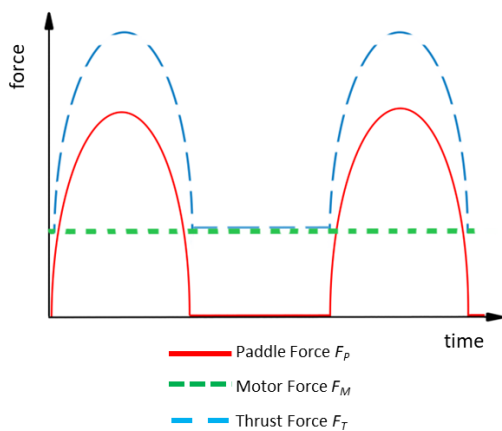


Figure 11: Strategy 1 - Constant support scheme.

The green line is the additional force F_M applied by the motor². The resulting force F_T from the paddle and motor is indicated by the blue line.

The aim of this strategy is to be as universal as possible for all requirements. It offers a compromise between dynamics and efficiency.

4.3 Strategy 2 - Direct Support

This strategy is based on the paddling rhythm of the user. Through the direct use of assistance, each paddle stroke is perceived as more powerful and the reaction of the boat as particularly dynamic³.

The strength of the assistance is aligned to the force measured at the paddle (F_P). The propulsion system replicates the force curve over a paddle stroke. As a result, the pushing force F_M should act synchronously with the paddle force F_P . The Fig. 12 shows the corresponding curve progression. It is special that the motor force has the same qualitative profile of the paddle force.

This strategy corresponds to the approach of a *pedelec* (elec. bicycle). Due to the simultaneous thrust of the drive, the paddle stroke should be potentiated and thus be perceived as more powerful.

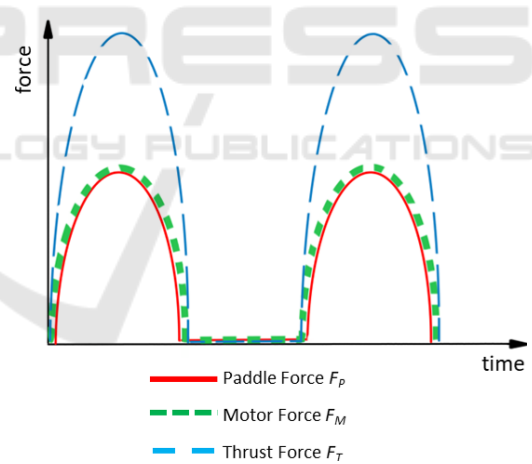


Figure 12: Strategy 2 - Direct support scheme.

4.4 Strategy 3 - Valley Support

In this strategy, the goal is to achieve high efficiency by moving the boat as smoothly as possible. The thrust of the motor F_M is used to supplement the paddling force F_P so that there is always a constant force on the boat. The maximum force to be supplemented is determined by the driver. Fig. 14 shows the progressions of the forces during paddling.

²Calculated from the averaged force of the paddle.

³The athlete has the impression of being much stronger.

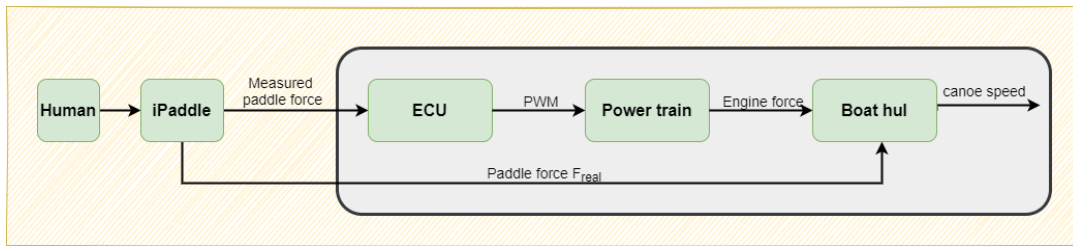


Figure 13: Basic structure of the simulation.

The advantage of this strategy is that the boat causes less dynamic motion and can therefore be driven more efficiently. The motor takes over the power requirements to propel the boat smoothly. The goal of this strategy is to eliminate speed fluctuations (Δv) as much as possible.

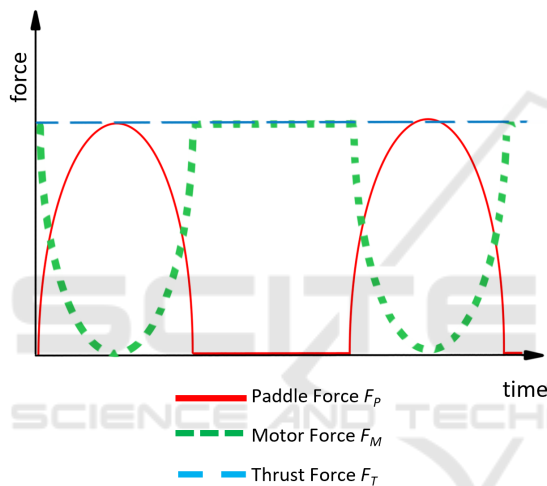


Figure 14: Strategy 3 - Valley Support scheme.

5 INVESTIGATING SUPPORT STRATEGIES USING A SIMULATION APPROACH

5.1 Aims and Principle Approach of the Simulation

One way to test the strategies mentioned above is to conduct real-life tests with the canoe. However, this requires a lot of technical and logistical effort. Another approach is to investigate the various support strategies using a holistic simulation approach. This makes it possible, for example, to identify errors in the actuation strategies in advance. This approach is significantly more efficient and saves resources.

Accordingly, the goal is to develop a physically

correct simulation model, for the investigation of the support strategies, in order to verify the presented approaches. Furthermore, the developed strategies can be transferred by a rapid prototyping approach, into C-code, which can be used directly in the microcontroller.

The simulation models are first developed with the assumption of ideal conditions. This means that there are no disturbing influences in the model. In reality, however, these always exist and include, for example, the influence of wind, currents and waves. Some of these influences can be approximated by constants, but deviations from the real system inevitably remain. These have to be estimated and evaluated.

The simulation and modeling of the entire system is realized with the program Matlab/Simulink from Math Works. The simulation consists of different blocks, each representing a sub-component of the overall system. The basic structure of the simulation model shown in Fig. 13 consists of several subsystems and is based on real conditions.

For example, the "Human" simulation block serves as input for the iPaddle model. The output variable paddle force is passed on as inputs to the "ECU" and "Boat hull" blocks. The ECU has the task of generating a PWM signal based of the revived sensor data, which is used to control the motor in Block "Power train".

The simulation results, especially the speed of the boat, can be validated with real measured values (e.g. with a GPS-sensor).

5.2 Realization of the Simulation

5.2.1 Model of the Boat Hull

The boat is a rigid body. To set it in motion a force must be applied:

$$a = \frac{F}{m} \quad (2)$$

where a is the acceleration, F is the total force acting on the body, and m is the mass of the body including the mass of the persons.

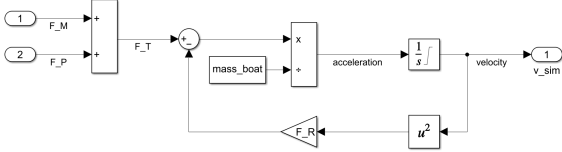


Figure 15: Signal flow diagram in Simulink (Seidel, 2022).

The speed of the boat is then obtained by integrating the acceleration to give:

$$v = \int a dt + v_0 \quad (3)$$

The force $F_{Forward}$ (F_F) results from all the partial forces (paddle force F_P , motor force F_M , resistance force F_R and thrust force F_T) acting on the boat to be:

$$F_F = F_P + F_M - F_R = F_T - F_R = m \cdot a \quad (4)$$

In a canoe, the force F_P results from the movement of the paddle in the water. An additional force F_M is generated by a motor used. These two forces combine to form the thrust force F_T . This is countered by a resistance force F_R , which depends, among other things, on the shape of the boat. Fig. 10 shows this situation on a canoe.

In order to create a simulation, it is therefore necessary to find out which input forces act on the boat through the paddle and motor and how the boat behaves in terms of the resistances that occur.

Modeling the physical behavior of a watercraft is very complex. In order to model the drag force as realistically as possible, a large number of physical equations and parameters must be considered. The total resistance of the boat is made up of several partial resistances, some of which are very complex to determine (e.g. skin friction resistance and pressure resistance, which can be further divided in *wake-making resistance*, *naked hull skin friction resistance* and so on).

The model can quickly become inaccurate and unrealistic because there are a large number of submodels for which assumptions have to be made. Therefore, the modeling is additionally supported by metrological investigations, e.g. by measuring the deceleration behavior. The model was created in Simulink according to equations 2, 3 and 4 with the signal flow diagram shown in Fig. 15.

For the determination of the boat resistance, the equation for the drag coefficient was used:

$$c_w = \frac{2 \cdot F_R}{\rho \cdot A \cdot v^2} \quad (5)$$

The c_w value, also called the drag coefficient, is composed of the density of the medium ρ , the face

area A , the velocity v of the incident flow of the medium and the drag force F_R .

In this context, the frontal area is the area that the respective medium, in this case water or air, impinges on in the direction of travel. The density of water is assumed to be constant at 1000 kg/m^3 and the density of air is assumed to be constant at 1.2 kg/m^3 .

Two fluids act on the paddler and the boat, on the one hand the air and on the other the water. Thus, after rearranging equation 5 and considering both fluids at once, the total drag force $F_{R,total}$ ($F_{R,t}$) results in:

$$F_{R,t} = F_{R,w} + F_{R,a} \quad (6)$$

Where the subscripts a and w stand for air and water and t for total, respectively. This gives the equation:

$$F_{R,t} = \frac{1}{2} \cdot \rho_w \cdot c_{w_w} \cdot A_w \cdot v_w^2 + \frac{1}{2} \cdot \rho_a \cdot c_{w_a} \cdot A_a \cdot v_a^2 \quad (7)$$

It is assumed for modeling purposes that there are no perturbations such as current or wind acting on the boat. The velocities of the inflow from air and from water are therefore equal to the velocity of the boat. Equation 7 can thus be simplified:

$$F_{R,t} = \frac{1}{2} \cdot v^2 \cdot (\rho_w \cdot c_{w_w} \cdot A_w + \rho_a \cdot c_{w_a} \cdot A_a) \quad (8)$$

It is difficult to capture the frontal area of the boat including the athlete and paddle⁴. For this reason, the factors K_w and K_a were used, which combine the unknown drag coefficient and the unknown frontal area of the respective medium. This results in the equation of the total resistance to be:

$$F_{R,t} = \frac{1}{2} \cdot v^2 \cdot (\rho_w \cdot K_w + \rho_a \cdot K_a) \quad (9)$$

After factoring out ρ_w , we get:

$$F_{R,t} = \frac{1}{2} \cdot v^2 \cdot \rho_w \cdot K \quad (10)$$

transformed, where:

$$K = K_w + \frac{\rho_a \cdot K_a}{\rho_w} \quad (11)$$

The parameterization of the model was determined using the deceleration behavior of the boat, similar to the usual procedure in automotive engineering. The magnitudes of the driving resistances are directly dependent on the velocity. In order to determine this relationship over the entire speed curve, a deceleration test was carried out.

⁴The area changes continuously during the ride, e.g., due to the continuous movement of the paddle, the sitting posture of the paddler, or the slight lifting out of the boat at higher speeds.

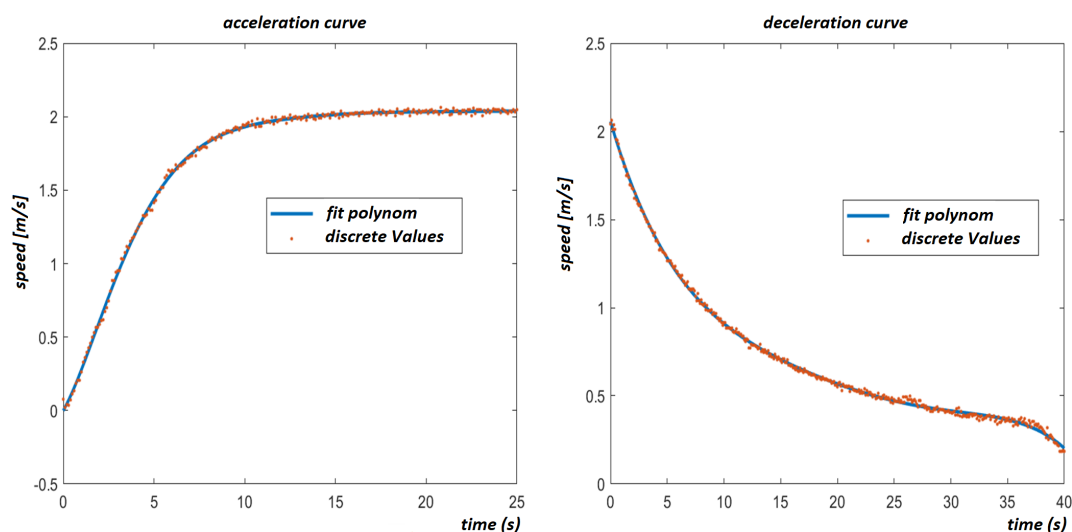


Figure 16: Acceleration and deceleration curve (Seidel, 2022).

The boat was accelerated to a given speed (e.g. 8 km/h) and then switched off. The drag forces acting on the boat result in a reduction of the boat speed until it comes to a standstill. Provided that no disturbance variables such as wind and current influence the behavior of the boat, the force acting on the boat can be calculated from the determined acceleration (respective negative acceleration).

The mass of the test vehicle was determined beforehand. Thus, the acting force F can be calculated at any time. The force and velocity can then be related via the time stamps. This experiment is carried out under the assumption that the resistance behaves identically at the same instantaneous speed - regardless of whether the boat is accelerating or moving at a constant speed. To obtain reliable values, the experiment is repeated several times and the mean value is calculated. With this procedure, the resistance from the speed could be determined.

Following the driving resistance determination of motor vehicles, the velocity curves of several deceleration curves of the boat were recorded for the determination of the force $F_{R,t}$. The acceleration was then calculated from the recorded velocities by derivation.

The acceleration and roll-out curves can be fitted 2nd or 3rd order polynomials. Therefore, an approximation of the real data is possible. An example comparison of the fitted and acquired data can be seen in Fig. 16. By the conversion into a continuous function a derivation is now possible. (Doblaski, 2021; Seidel, 2022; Vikulin, 2021)

5.2.2 Model of the Paddle

Once the boat model has been validated, a "standard paddle stroke" for amateur athletes must be defined and converted into a functional block for comparative studies. To do this, the maximum force must first be determined and specified.

Fig. 18 shows forces on kayak paddles during use by competitive athletes. The forces are plotted in newtons for women's (F) and men's (M) rides at different paddle cadences in strokes per minute (spm). The force of a female athlete at 60 spm, corresponds to forces of up to 126 N. This defines the maximum values.

The acquired force on the paddle is not fully used for propulsion. The captured force must be corrected with a paddle function. For initial assumptions, a paddle factor should suffice for now.

The paddle factor depends, among other things, on the blade shape. Symmetrical paddles have an efficiency factor of up to 74 %, asymmetrical paddles up to 89 %. The paddle used for the tests is highly asymmetrical. Both the paddle angle and the paddle distance from the boat have also a large influence on the effective propulsive force (Jackson, 1995; Vikulin, 2021). To reduce the number of unknown variables, a very accurate paddle guidance is assumed.

To capture the correct paddle factor, real measurements of the paddle are given to the validated boat model and fitted until the curves match sufficiently accurately. Fig. 17 shows the measured data of the left and right paddle as well as the resulting force acting on the boat through the paddle as propulsive force. The measurements were made on a lake near by Dresden under good weather conditions (only light



Figure 17: Boat hull validation.

wind). Special measurement equipment from Lord ZSE Electronic was used for the tests. The speed recording is based on a satellite-based measurement like GPS.

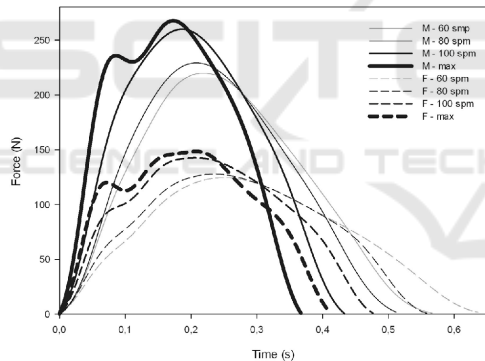


Figure 18: Force applied to kayak paddles by competitive athletes by paddle frequency and gender (Gomes et al., 2015).

5.2.3 Model of the Power Train

The control of the motor is realized by pulse width modulation (PWM). The calculated duty cycle of the desired PWM signal is transferred to the motor controller via a microcontroller. This is housed with the battery and the drive in the drive train subsystem (Fig. 1). The motor controller controls the motor, which generates a force in the longitudinal direction via the impeller on the drive shaft. As a further input, the boat subsystem also has the force of the paddle, which also drives the boat.

From the calculation for the jet model, it is known

that the thrust depends on the rotational speed as well as the difference between the ejection and inflow velocities. In order to determine this relationship in a way that could be used for the model, several test runs were carried out and the results were then stored in the form of a characteristic diagram. This means that the drive model can be treated as a black box.

5.3 Validation of the Simulation

The vehicle model consists of subsystems of different types and behavior, which requires a separate approach (simulation approach) depending on the part model (sub-model). To meet the requirements of a complete vehicle simulation (integration of ECUs, consideration of physical behavior, use of analog controllers), a hybrid simulation approach or co-simulation must be used.

Fig. 20 shows the complete simulation model, based on the block diagram in Fig. 1. In addition, the "ECU" and "User Input" block has been added. The control algorithms are implemented in the "ECU" and possible user inputs are processed in the "User Input" block.

To validate the simulation, the force of the paddle acting for propulsion is applied to the boat model and then the resulting simulated speed is compared with the real recorded speed. Since the recorded force of the paddle (see also section 5.2.2) does not act directly as a propulsive force, an adjustment was made using a paddle factor.

The aim is to simulate the real speed as accurate as possible using the Simulink model. If the course of the real speed matches the simulated speed suffi-

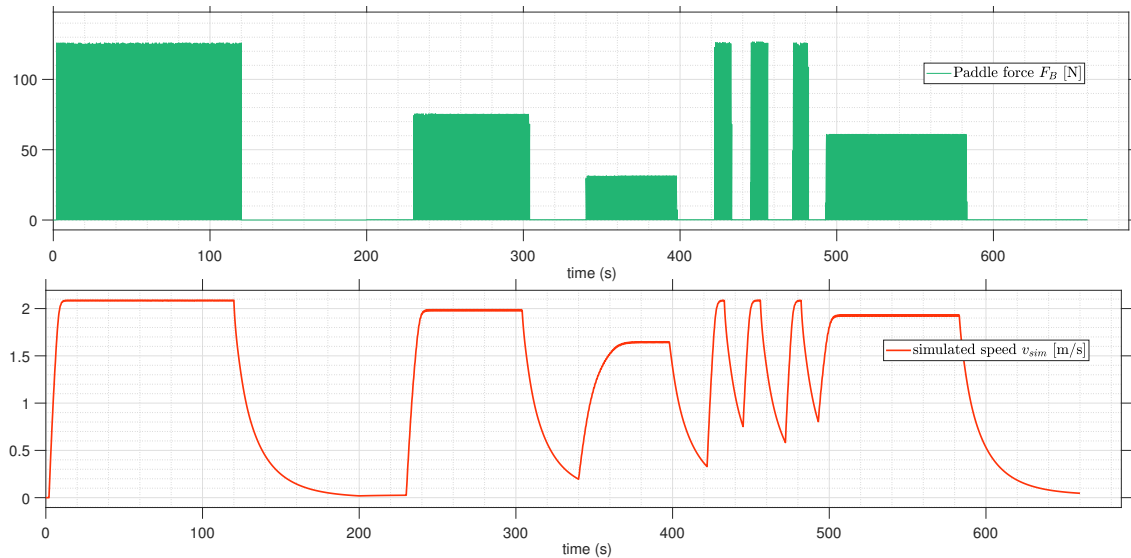


Figure 19: Htw Dresden paddle cycle for analyzing *paddelec* support strategies.

ciently accurate, the simulation model has been parameterized correctly and can be used for further investigations.

Fig. 17 shows an example of a measurement run that was used to validate the simulation model. The respective left and right paddle forces are shown at the top left and right. These are the measured force F_B on the paddle. In the lower picture, the measured velocity is shown in green (V_{meas}) and the result of the simulated velocity in blue (V_{sim}).

In the initial range of the measurement (1-60 seconds) clear deviations can be seen, which can be explained by wind influence. The remaining course of the simulated speed agrees very well with the measured one. Thus, the model can be accepted as validated for this individual case.

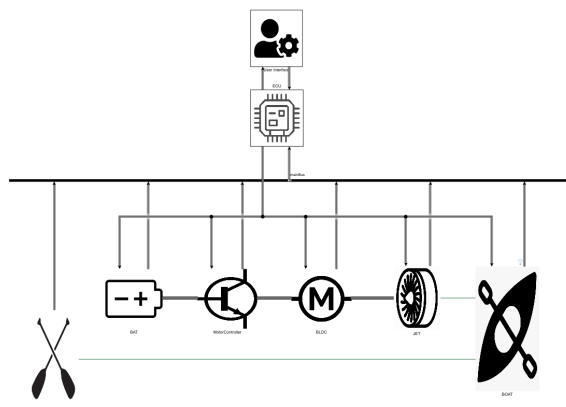


Figure 20: Structure of the overall simulation.

5.4 Simulation Results

5.4.1 Paddle Cycle for Testing Support Strategies

A paddle cycle of about 10 minutes is used to investigate the different strategies. To vary the paddle strokes, the maximum value is scaled. The paddle frequency is not changing over time. Fig. 19 shows the progression. First, the athlete paddles with the synthetically generated simulated "norm paddle stroke for amateur athletes" for about 120 seconds with 100 % of the specified maximum force of 126 N (F_B). Afterwards there is a ca. 2-minute break. Then the athlete paddles for 70 seconds with 60 %, makes a break of 40 seconds and returns to paddle with 25 % of the specified maximum force. After another short break, there are 3 fast paddle cycles of ca. 10 seconds followed by a constant phase of 50 % (90 seconds). The cycle runs until the canoe stops.

The lower section of the figure shows the simulated behavior of the boat without the influence of disturbance variables or support forces. A maximum speed of approx 2.1 m/s is achieved.

5.4.2 Comparison of the Strategies

Fig. 21 (upper plot) shows the velocity profiles with the application of all three strategies explained before. The paddle profile from Fig. 19 was used for the simulation. The lower plot shows the additional forces added by the motor. The green curve (dotted line) shows the velocity profile without additional support.

It is noticeable that the thrust assistance has a

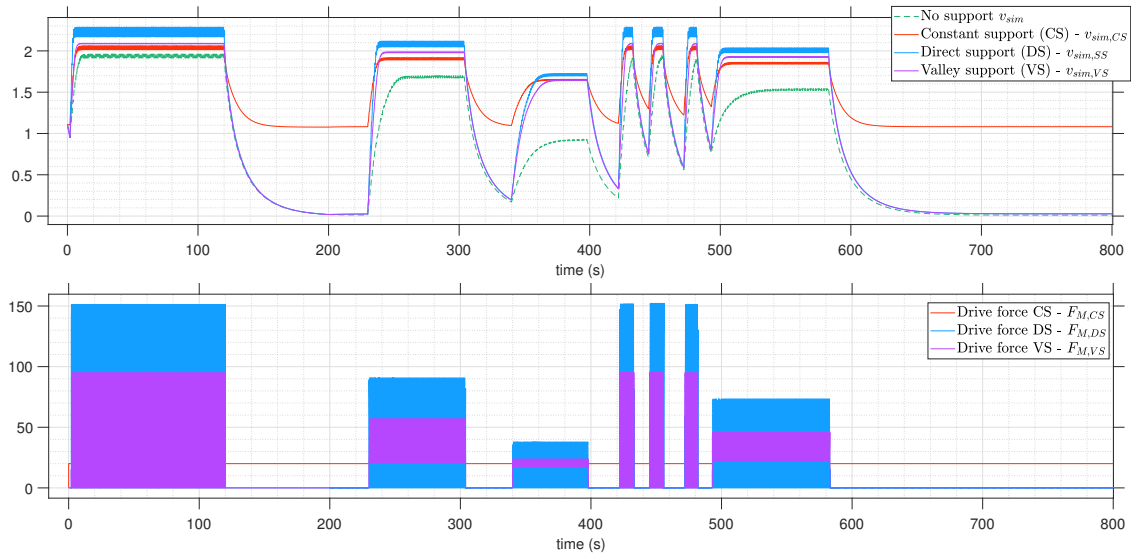


Figure 21: Simulated speed curves of different support strategies.

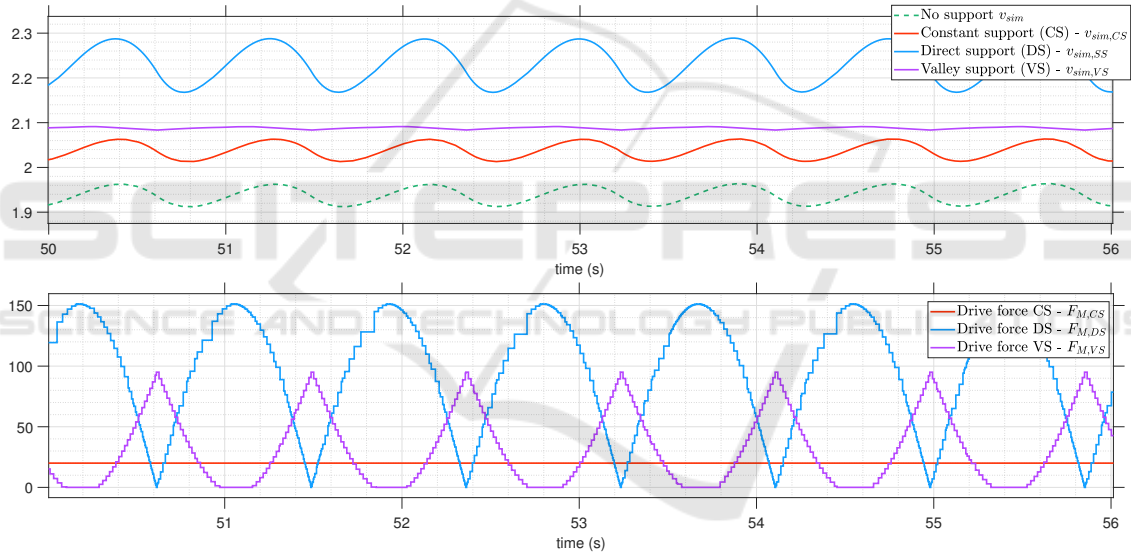


Figure 22: Zoomed curves from figure 21.

greater effect at lower speeds. A significant speed difference at maximum paddle force is hardly noticeable. In order to see a large change here, a more powerful power train is needed, since the speed enters quadratically into the resistance calculation (see also equation 10). However, this does not make sense for the envisaged canoeing, since it also means that a larger battery is needed and correspondingly heavier drive components. An acceptable compromise must be found here.

In Fig. 22, the time course from graph 21 is zoomed in. So that the different behavior of the strategies can be seen better. The purple curve $v_{sim,VS}$ shows a very smooth speed curve, which is achieved

by a correspondingly dynamic control of the drive in the valleys ($F_{M,VS}$). The red curve $v_{sim,CS}$ corresponds to the original curve without support but with a given offset. The blue curve $v_{sim,DS}$ shows the largest changes in velocity and is therefore also the worst in terms of energy. However, it can be assumed that this mode is perceived as very dynamic and met with great approval.

6 CONCLUSIONS

The fundamentals of an intelligent paddle (iPaddle) and its suitability as a control device for electric aux-

iliary drives were investigated.

The behavior expected in advance in terms of thrust could be confirmed in principle. In the future, the use of an optimized waterjet drive is planned. The main aim is to reduce propulsion losses and to integrate the propulsion system into the hull of the boat in a form-fit manner.

Extensive hardware and software tools were created for the metrological investigation of an electrically assisted canoe.

A new simulation model of the longitudinal dynamics was developed. The drive train and driving resistance subcomponents were modeled in the form of a black box using the measurement data from driving tests. This can be used among others to test the support strategies in the laboratory.

The realistic behavior of the overall simulation was examined and evaluated using an extensive test scenario. The basic strategies can now be further supplemented and examined with the aid of the simulation. The theoretically elaborated strategies could partly be tested practically on the water.

By means of recorded data of the measurement runs, further investigations can be carried out on the boat, e.g. the influence of disturbance variables.

With the evaluation of the practical testing, it could be shown that some support strategies behave significantly different in reality than was assumed theoretically.

The use of a position sensor for the iPaddle is currently being investigated to measure the position in space more accurately. This will make it possible to develop more precise strategies and implement new safety features, such as preventing the motor from being supported in certain situations like special course corrections.

REFERENCES

- Aentron (2022). Energy solutions.
- BMW (2013). Water tourism in Germany.
- Doblaski, J. (11/2021). *Investigation of model-based actuation strategies for an electrically powered kayak*. Diploma thesis, HTW Dresden, Dresden.
- Dr. Budich, R. and Dabrazzi, E. (2020). Drive system for a watercraft that can be moved by muscle power, and method for controlling a drive system.
- Gomes, B. B., Ramos, N. V., Conceição F, A. V., Sanders, R. H., Vaz, M. A., and Vilas-Boas, J. P. (2015). Paddling force profiles at different stroke rates in elite sprint kayaking. *Journal of applied biomechanics*, 31(4):258–263.
- Häse, M. (04/2020). *Investigation of sensors for force mea-*

surement in electrically assisted canoeing. Diploma thesis, HTW Dresden, Dresden.

Hauptmann, F. (05/2020). *Simulation, analysis and control of the electric drive train of a watercraft*. Diploma thesis, HTW Dresden, Dresden.

Jackson, P. S. (1995). Performance prediction for olympic kayaks. *Journal of sports sciences*, 13(3):239–245.

Kaitts Ltd. (2022). Online shop.

Kedean (2022). Online shop.

Pöschmann, M. (05/2020). *Development of a modular energy storage and management system for LEVs (light electric vehicles)*. Diploma thesis, HTW Dresden, Dresden.

Seidel, J. (02/2022). *Analysis of paddle and motion data of an electrified kayak and optimization of the measurement system*. Diploma thesis, HTW Dresden, Dresden.

Vikulin, A. (11/2021). *Contribution to the modeling and control of a hybrid driven stand-up paddle*. Master thesis, HTW Dresden, Dresden.